DERIVATION OF A QUANTITATIVE KINETIC MODEL FOR A VISUAL PIGMENT FROM OBSERVATIONS OF EARLY RECEPTOR POTENTIAL

B. MINKE, S. HOCHSTEIN, *and* P. HILLMAN

From the Institute of Life Sciences, The Hebrew University of Jerusalem, Jerusalem, Israel

ABSTRACT   A "complete" and quantitative kinetic model for the states and transitions of the barnacle visual pigment *in situ* has been constructed from intracellular recordings of the early receptor potential responses to long light pulses. The model involves two stable and four thermolabile states and 10 photochemical, thermal, and metabolic transitions among them. The existence of each state and transition is demonstrated by qualitative examination of the response resulting from a carefully chosen experimental paradigm (combination of intensity, duration, and wavelength of adaptation and stimulation). Quantitative examination of the same responses determines all of the model transition rates, but only puts constraints on the state dipole moments. The latter are determined, and the former refined, by quantitative comparison of the predictions of the complete model with the responses to a set of paradigms chosen to involve as many states and transitions as possible. The fact that good fits can be obtained to these responses without further modification of the model supports its completeness.

I. INTRODUCTION

A number of kinetic models have been worked out for the changes occurring in the visual pigment molecule following the absorption of a photon (reviewed by Morton, 1972; Abrahamson and Wiesenfeld, 1972; and Kropf, 1972). These models have been derived, in general, from spectrophotometric studies on visual pigments in detergent solutions, although more recently, some (partial) *in situ* results have been reported (see Abrahamson and Wiesenfeld, 1972 and also Brown and White, 1972). It is now accepted that the early receptor potential (ERP) is generated by charge displacements produced directly by conformational changes in the dipole moment of the molecule. Thus the ERP is a linear measure of pigment change and may be used for studying the pigment cascade (Arden et al., 1966; Cone, 1967; Pak and Boes, 1967; Hagins and McGaughy, 1967; Ebrey, 1968). In both spectrophotometric and ERP studies, brief bright flashes of light have been used to determine the photosensitivity or absorption spectrum at a particular time, and the transition rates be-

tween the stages or states were usually derived from changes in these measures with time.

We now report the systematic construction of a "complete" and quantitative pigment transition model for the barnacle visual pigment from the ERP responses of the photoreceptors to long light pulses. The model is built up step by step: at each step a new experimental paradigm results in a response whose interpretation requires the addition of a new transition or state to the model.

The completeness of the resulting model is witnessed by the fact that the response to further paradigms, chosen to be as complex as possible (that is, to involve as many states and transitions in as many combinations as possible), can be quantitatively fitted by the model without further modification. However, neither completeness nor uniqueness can of course ever be proven, and there may well be very short-lived intermediates (like prelumirhodopsin) which would not have been seen.

All of the transition parameters are directly determinable by quantitative analysis of the same experiments used to determine the existence of those transitions. The (relative) state dipole moments are determined, and the transition parameters refined, in the process of optimalization of the fit of the calculated model predictions to the responses to the complex paradigms of the preceding paragraph.

The calculations of the predicted responses were done numerically by a computer. The model parameters were varied for best fit in each cell (and at each temperature) subject to theoretical constraints (following section) as well as experimental constraints (direct measurements and comparisons with other cells, see section III).

The use of long pulses of light (in addition to short) appears to have certain advantages. The most obvious is the separation of "on" and "off" transients. The latter directly determine the products of the dipole moment changes in the transitions and the photosensitivities and instantaneous populations of the thermolabile states.

The visual pigment was that of the lateral ocellus of the barnacles *Balanus amphitrite* and *eburneus*, which has been shown to be of particular interest in having two dark-stable states (Minke et al., 1973). No significant differences were observed between the two species, which are therefore not separately identified in this paper, their pigments being assumed identical.

II. METHODS

Experimental Techniques

Intracellular recordings were made in excised photoreceptors of the barnacles *Balanus eburneus* and *amphitrite* as described elsewhere (Hillman et al., 1973; Minke et al., 1973). Again, the quantitative ERP measurements of this report were obtained from cells in which the late receptor potential (LRP) had disappeared spontaneously. In this condition, the input time constants of the cells, measured from the response to a square wave of applied current, were in the range 0.5–2.0 ms. The unfiltered light intensity at the photoreceptor was about 1×10^{16} photons/cm² per s per nm at 550 nm. Table I gives the wavelength charac-

TABLE I
FILTER AND LIGHT CHARACTERISTICS

Filter	Peak wavelength	Full width at half height	Full intensity at photoreceptor
	nm	*nm*	*photons/cm²/s* $\times$ *10¹⁶*
K3	495	45	12
K5	600	50	50
K6	650	55	43
447	447	8	0.7

teristics and calculated full intensities for each color filter used. All intensities used were the maximum available (defined as log I = 0) except where otherwise noted. We estimate that the light intensity was reproducible from experiment to experiment within about a factor 2, the uncertainty arising mainly from geometrical factors.

Mathematical Procedure for Computer Model

The model which will be developed relates to a system of identical noninteracting molecules each having several states among which there are various thermal and photochemical transitions.

Symbols Used

$A(t)$, $B(t)$, $C(t)$ $\cdots$ Fraction of molecules in the various pigment states at time t (abbreviated A, B, C, $\cdots$).

k_{BA} Rate of thermal transition from A to B (fraction of molecules in state A per ms).

IX_{BA} Rate of photochemical transition from A to B (fraction of molecules in state A per ms), where

I Light intensity (photons/cm² per ms), and

$X_A = X_{BA} + X_{CA} + \cdots$ Photosensitivity of state A (cm²/photon).

M_A Dipole moment of state A.

$\dot{V}(t)$ Time derivative of the total potential due to pigment dipole moment changes at time t.

$\dot{V}_A(t)$ Contribution of time derivative of A to $\dot{V}$ at time t.

τ_m Input time constant.

$ERP(t)$ Computed early receptor potential.

Differential Equations

$$\dot{A} = -(k_{BA} + k_{CA} + \cdots + IX_{BA} + IX_{CA} + \cdots)A$$
$$+ (k_{AB} + IX_{AB})B + (k_{AC} + IX_{AC})C + \cdots$$

$$\dot{B} = (k_{BA} + IX_{BA})A - (k_{AB} + k_{CB} + \cdots + IX_{AB} + IX_{CB} + \cdots)B$$
$$+ (k_{BC} + IX_{BC})C + \cdots$$

$$\vdots \tag{1}$$

$$\dot{A} + \dot{B} + \cdots = 0 \tag{2}$$

$$A + B + \cdots = 1 \tag{3}$$

$$\dot{V}_A(t) = \dot{A}(t)M_A$$
$$\dot{V}_B(t) = \dot{B}(t)M_B$$
$$\vdots \tag{4}$$

$$\dot{V}(t) = \dot{V}_A(t) + \dot{V}_B(t) + \cdots \tag{5}$$

$$\text{ERP}(t) = \int_0^t \dot{V}(t')e^{(t'-t)/\tau_m}\, dt'. \tag{6}$$

Assumptions

(*a*) The pigment system is closed, i.e. the total number of pigment molecules is conserved (Eq. 3; also implied in Eqs. 1 and 2).

(*b*) All pigment transition rates are first order, i.e. they are independent of the populations of the states. (In Eq. 1 the k's are state-population independent.)

(*c*) The dipole moments and photosensitivities are fixed and universal, i.e., they are the same in all cells and are independent of time, temperature, or state populations. (In Eq. 1 the X's and in Eq. 4 the M's are constants.)

Numerical Solution

Eqs. 1 and 3 are first solved analytically for the steady-state condition during illumination ($\dot{A} = \dot{B} = \cdots = 0$). Then the dark adaptation populations are found by solving Eqs. 1 and 3, if necessary numerically ($\dot{A} \rightarrow \Delta A/\Delta t$, $\dot{B} \rightarrow \Delta B/\Delta t$, $\cdots$; $A(t) = A(t - \Delta t) + \Delta A(t)$, $B(t) = B(t - \Delta t) + \Delta B(t)$, $\cdots$) keeping $I = 0$ and using the steady-state populations found above as the initial populations ($A(0)$, $B(0)$, $\cdots$). Finally, the pigment-state relative populations during and following a test stimulus are found by re-solving the equations numerically, using now these dark adaptation populations as the initial populations and setting I appropriately for the intensity and duration of the light stimulus. The resulting populations then lead to the theoretically expected early receptor potential by the finite-step equivalents of Eqs. 4–6:

$$\Delta V_A(t) = [A(t) - A(t - \Delta t)]M_A , \tag{7}$$

$$\Delta V(t) = \Delta V_A(t) + \Delta V_B(t) + \cdots , \tag{8}$$

$$\text{ERP}(t) = \text{ERP}(t - \Delta t)e^{-\Delta t/\tau_m} + \Delta V(t), \tag{9}$$

where $\text{ERP}(0) \equiv 0$.

III. STEPWISE BUILDING OF A PIGMENT-KINETICS MODEL FROM THE ERP OBSERVATIONS

A. *Two Dark-Stable States*

Minke et al. (1973) have shown that the pigment responsible for the ERP in the barnacle may exist in two states which are stable in the dark. Furthermore, the

absorption spectra of the two states differ, with maxima at 532 and 495 nm, respectively, so that a net transfer of pigment may be induced by excitation with colored stimuli. We call these states A and D, respectively. Substantial activation of state A (red stimulation following blue or white adaptation) induces a negative ERP (hyperpolarizing); and of state D (blue or white stimulation following red adaptation), a positive ERP. A white stimulus following white adaptation induces a mixed response which is biphasic (positive first) at low temperatures, where the phases are sequential. We may thus assign to state A a dipole moment of zero and to state D, -1.0. (Since the values are only relative and in arbitrary units, only the sign is significant.)

B. Dark Recovery

Hillman et al. (1973) have shown that following a bleaching white stimulus both the negative and (since the biphasic shape of the response does not change strongly during the recovery), the positive ERP's recover exponentially with similar, strongly temperature-dependent rates ($1/e$ time constants of 80 ms at 24°C and 1,800 ms at 4°C; i.e. a Q_{10} of about 4.7). We assume both these recovery transistions to originate from a single pigment state which we call F, and that these are the fastest transitions from that state. The conclusions of sections A and B are summarized in Fig. 1.

C. Photosensitivities of the Dark-Stable States

The photosensitivity of a state is the cross-section for photon absorption by a molecule in that state. The rate constants (photosensitivity X times light intensity I) of the two stable states were always measured in the same cell, so the measured *ratio* of the rate constants was independent of the uncertainty in the absolute light intensity. Figs. 2 and 3 show examples of measurements from one cell for the A and the D states, respectively. The measurements were carried out at low temperature (5°C) to slow the return of the pigment to the other state by way of the dark recovery. The cell was blue adapted in Fig. 2 or red adapted in Fig. 3 and then exposed to pairs of pulses of red (K5) light in Fig. 2 or blue (K3) light in Fig. 3. The first pulse was of variable duration, to excite a variable amount of pigment, while the
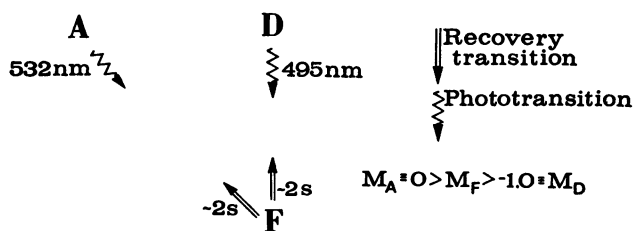

FIGURE 1 The minimal model needed to explain the observations of sections A and B. The numbers adjoining the phototransitions indicate the wavelengths of the peaks of the respective states of origin. The numbers adjoining the other transitions indicate the approximate time constants of these transitions at low temperature.
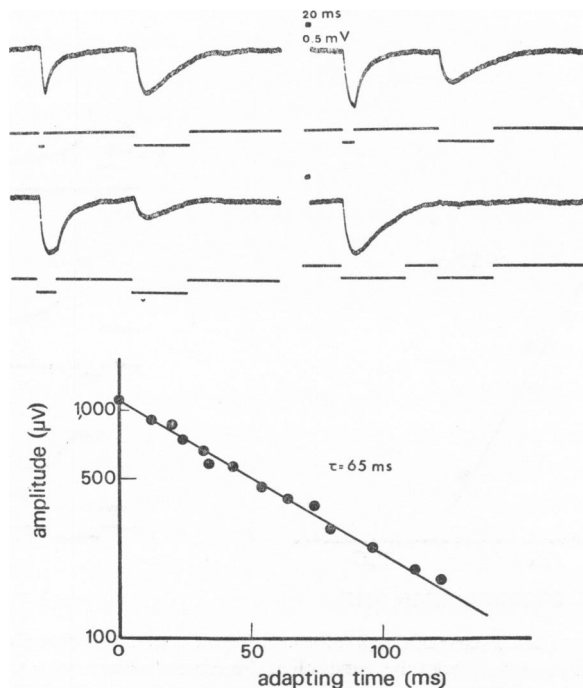
FIGURE 2 The rate of decrease of the population of the A state. The cell (at 5°C) was initially blue-adapted (447 nm, 10 s) and 30 s later exposed to two red (K5) pulses. The first (adaptation) pulse was of variable duration while the second (test) pulse was of fixed duration. Four examples of the responses to the red pulses are shown. The logarithm of the amplitude of the peak of the second response (which is a measure of the residual A-state population) is plotted against the durations of the adapting pulses in the graph. All points are derived from the same cell. The straight line denotes an exponential decay with $1/e$ time constant of 65 ms. The light duration is indicated by the photocell response below each trace in this and all the following figures. A calibration pulse precedes the responses in most figures.

second was of fixed duration and served to test the remaining pigment population. Since the test pulses activate only one state we expect the *shape* of the responses to be the same in all cases and only the amplitude to change. The amplitude (at peak) is plotted (on a logarithmic scale) against the duration of the first, adapting pulse. In both figures, the plot shows that the population does decrease exponentially with adapting duration, and with $1/e$ time constants of 65 and 22 ms, respectively, at these light intensities (see Table I). Extrapolating from the wavelengths used to the absorption spectrum peaks, we obtain photosensitivities $X_A(532 \text{ nm}) = 0.9 \times 10^{-16}$ cm²/photon and $X_D(495 \text{ nm}) = 3.7 \times 10^{-16}$ cm²/photon. The value of X_A is similar to, and that of X_D rather higher than, visual pigment sensitivities measured in situ and in vitro in other animals as quoted by Dartnall (1972) but both are lower than the figure derived by Mainster and White (1972) from Cone's (1963) measurements in the rat.
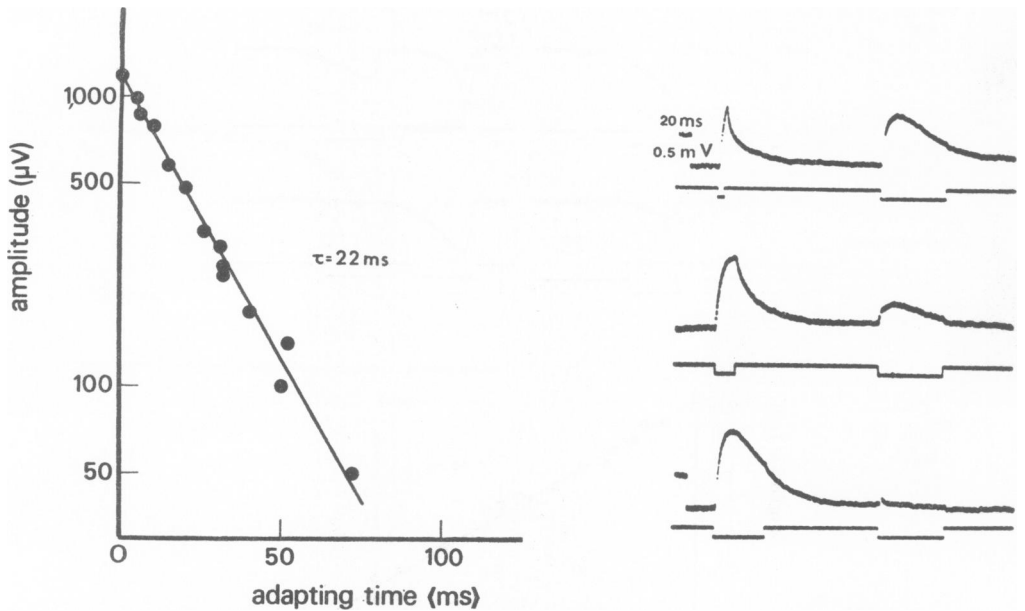
FIGURE 3 The rate of decrease of the population of the D state. The procedure is exactly as in Fig. 2 (and the results are from the same cell at the same temperature), except that the cell was initially red adapted (K6, 10 s) and 30 s later was exposed to two blue (K3) pulses (examples of responses illustrated). The straight line indicates a $1/e$ time constant of 22 ms.

D. *The Negative ERP Pigment Subsystem*

Fig. 4 shows, on a fast sweep speed, that there is a definite latency in the response to red stimulation which activates only the negative-ERP-producing A state. This latency is about 1 ms at 24°C, increasing to 3 ms at 9°C, and probably cannot be explained by a cancellation due to a simultaneous positive ERP, as only the A state is activated by the red stimulus. This, together with the temperature dependence of the latency, make it clear that the negative ERP is produced by a thermal transition originating from a pigment state populated by photoactivation of the A state. We call this new state B.

The upper right trace of Fig. 4 shows, however, that one thermal transition is not enough to explain the negative ERP shape. If the stimulation runs through a small part of the A state population, after the light is turned off there is a continued depolarization with at least two decay time constants (see graph below trace). These time constants cannot be either the input time constant, which is generally less than 2 ms (see following section for direct evidence in this cell) or the recovery time constant, which is about 2 s. There are thus two additional thermolabile pigment states which intervene between the stable state A and the state F responsible for the recoveries. These states are B and a new one we call C. Since the initial phototransition induces no ERP the dipole moment of B must be zero and, since both produce
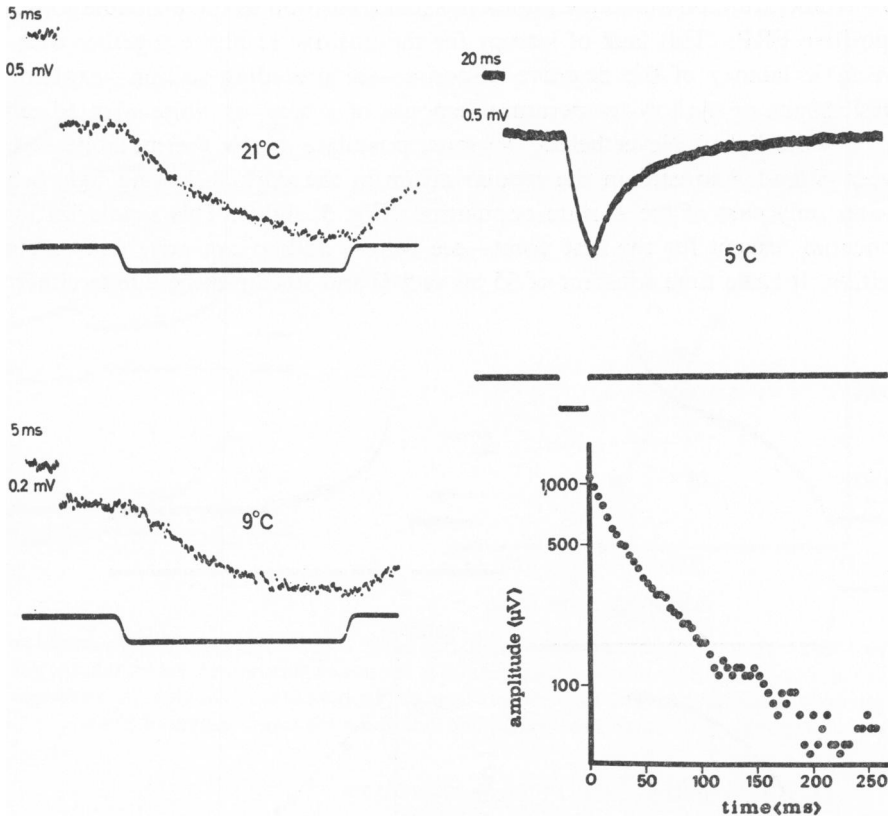
FIGURE 4   The thermal transitions producing the negative ERP. The traces in the left column show responses to red (K5) stimulation 30 s after blue (447 nm, 10 s) adaptation in one cell at two different temperatures. The figure shows that there is a latency of about 1 ms at 21°C and about 3 ms at 9°C. The upper right trace of Fig. 4 shows the response at 5°C (in another cell) to brief red (K5) stimulation 30 s after blue (447 nm, 10 s) adaptation. The decay of this response following cessation of the light is displayed on a logarithmic amplitude scale in the graph. The graph shows that at least two time constants are necessary to fit the negative ERP decline.

negative ERP's, the dipole moment of C must be between zero and that of F (see Fig. 6).

E. *The Positive ERP Pigment Subsystem*

Prolonged red adaptation brings nearly all the pigment molecules to the D state (Minke et al., 1973). Activation with a following white light produces a positive ERP with a latency of less than about 0.6 ms at both high temperature (24°C, Fig. 5, top left) and low temperature (10°C, Fig. 5, bottom left). The lack of latency[1] even

---

[1] A temperature-dependent latency of a few 10ths of a millisecond cannot be excluded by present data. This would indicate the existence of a short-lived intermediate between D and E with the dipole moment of D.

at low temperature points to the photochemical transition as the probable source of the positive ERP. (This lack of latency for the positive response together with the appreciable latency of the negative response—see preceding section—explain the biphasic shape of the low-temperature response of a blue- or white-adapted cell to blue or white light.) Nevertheless, we must postulate a new thermolabile state E between D and F to explain the repolarization in the dark following light which activates only part of the D-state population (Fig. 5, right). This repolarization is exponential (except for the first point—see below) and so can arise from a single transition. It has a time constant of 35 ms at 5°C and so cannot be due to either the
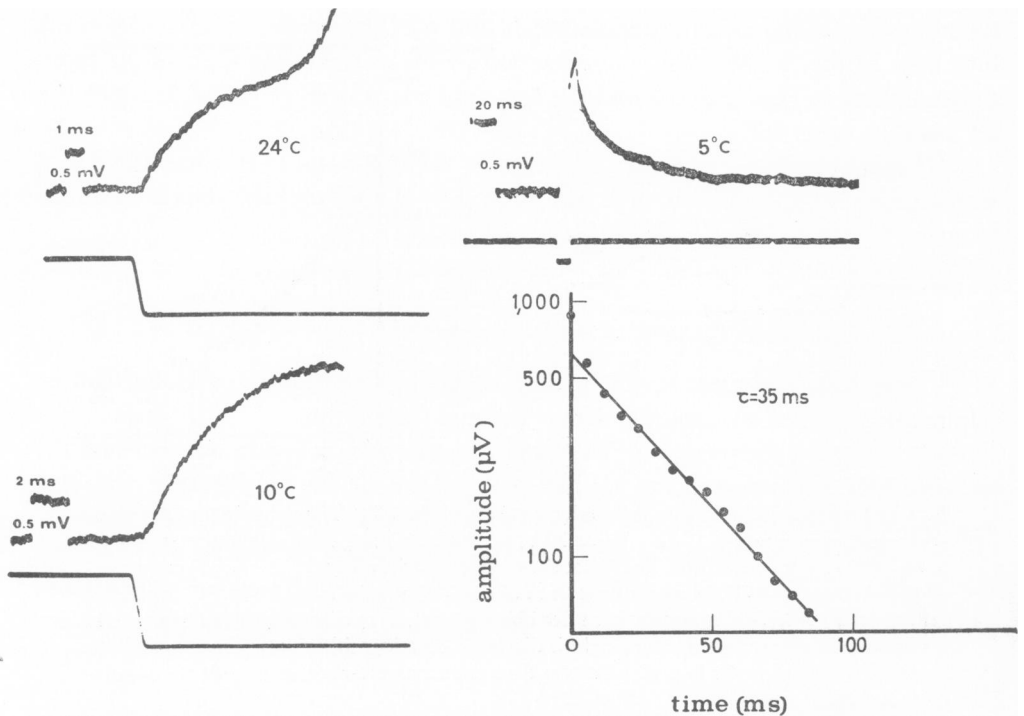

FIGURE 5 Thermal transition contributing to the positive ERP shape. The left traces (in the same cell) represent responses to maximum white light stimuli 30 s after blue (447 nm, 10 s) adaptation. Both responses have latencies of less than about 0.6 ms. (The last part of the first trace shows the initial effects of the LRP, which was still present in this cell.) The upper right trace shows the response of another cell to blue (K3) stimulation 30 s after red (K6, 10 s) adaptation. The blue stimulation runs through about 35% of the D-state population (see Fig. 3). The decay of this response following cessation of the light is displayed on a logarithmic amplitude scale in the graph (filled circles). The straight line represents a time constant of 35 ms. The deviation of the first point from the straight line is reduced when the blue pulse is lengthened. With stimuli long enough to run through all the pigment population this point falls on the straight line. This graph shows that in addition to the photochemical transition from the D state, which manifests itself as a rapid decay at the cessation of the light for short-pulse stimulation, another thermal transition is needed in order to explain the shape of the positive ERP.

input time constant (2 ms) or the dark recovery (2 s). It also has a weak temperature dependence ($Q_{10} = 2.5 \pm 0.3$).

The deviation of the first point in the graph of Fig. 5 from the straight line indicates the existence of an additional very fast time constant in the ERP repolarization. The source of this additional time constant becomes clear if we study the positive ERP following longer blue pulses (as in Fig. 3, same cell). The deviation of this point decreases with increasing stimulus duration, and the point falls on the straight line when the blue light runs through nearly all the D-state population (see graph, Fig. 3). Thus, this additional time constant, whose value is less than 2 ms, apparently derives from the cessation of the D-state activation, integrated by the membrane time constant. (The D-state population is still 60% of maximum after the short blue light of Fig. 5.) We may, therefore, take 2 ms as the upper limit of the input time constant in Figs. 2 and 3 and the top right traces of Figs. 4 and 5, which are all from the same cell.

Note that the *absence* of such a deviation of the first point in the graph in Fig. 4 strengthens the suggestion that the transition $A \rightsquigarrow B$ involves little change of dipole moment.

The conclusions of these sections are summarized in Fig. 6.

F. Transitions Connecting the Subsystems

The experiments described in this section require no additional states but can be minimally explained by addition of four thermal transitions.

The experiment shown in Fig. 7 indicates that there is a fast transition from the negative ERP subsystem to the positive one: the cell, at low temperature, was blue adapted and then exposed to two light pulses, the first red, shifting pigment from the A state without simultaneously activating the D state, and the second white, to test the D-state population after different dark times. Clearly, most of the pigment arrives at the D state within 100 ms or so and therefore not by the recovery transition.
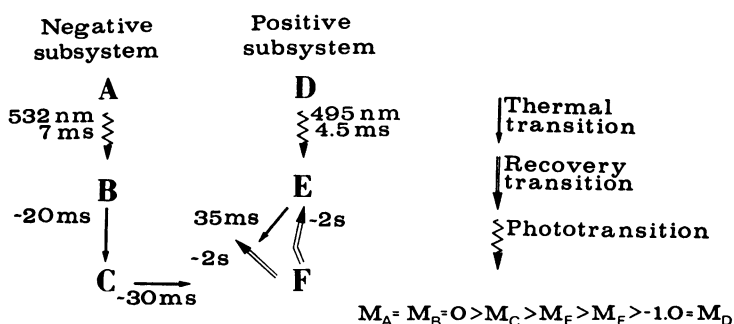

FIGURE 6 The minimal model needed to explain the observations of sections A–E. The second numbers adjoining the phototransitions indicate the approximate time constants of these transitions in full white light.
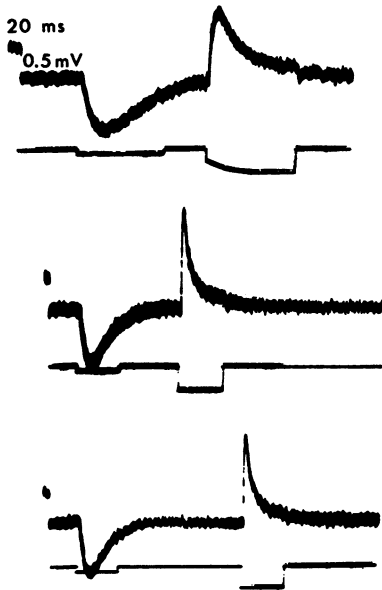
FIGURE 7 Fast transition from the negative to the positive ERP subsystem. All responses are from one cell at 3°C exposed to two light pulses 30 s after blue (447 nm, 10 s) adaptation. The first pulse of each pair was red (K5) and the second white. The size of the positive response to the white pulse is a measure of the D-state population. The figure shows that most of the pigment shifted by the red pulse out of the A state arrives at the D state within about 100 ms. The three traces are at the same gain but the last two are at half the sweep speed of the first.

Thus, there is a transition from the negative ERP subsystem to D, say $C \rightarrow D$ ($B \rightarrow D$ is also possible).

Furthermore, the recovery transitions from F have approximately equal rates (Hillman et al, 1973). At high light intensities, most of the pigment is in F in the steady state, since the lifetimes of all the other states are much shorter when the light is on. The dark population following long bright lights should therefore be about equally divided between A and D. In the specific cell illustrated in Minke et al. (1973) the recoveries were indeed closely equal, while 80% of the pigment following bright white lights was shown to be in A. This discrepancy must be due to the diversion to A of part of the $F \rightarrow D$ recovery. This means that the $F \rightarrow D$ recovery must go via B or C and that B or C have transitions to F. We choose C as the intervening state, so that the new transitions are $F \rightarrow C$ and $C \rightarrow F$.

The existence of the transition $C \rightarrow F$ also manifests itself in the impossibility of transferring nearly all of the A population to D by exposure to a red light whose amount is calculated to be sufficient to run through almost all of the A population once; much more red light is needed to empty A nearly completely.

The experiment in Fig. 8 shows, on the other hand, that there is *no* fast transition from the positive to the negative subsystem. The responses shown are to pairs of
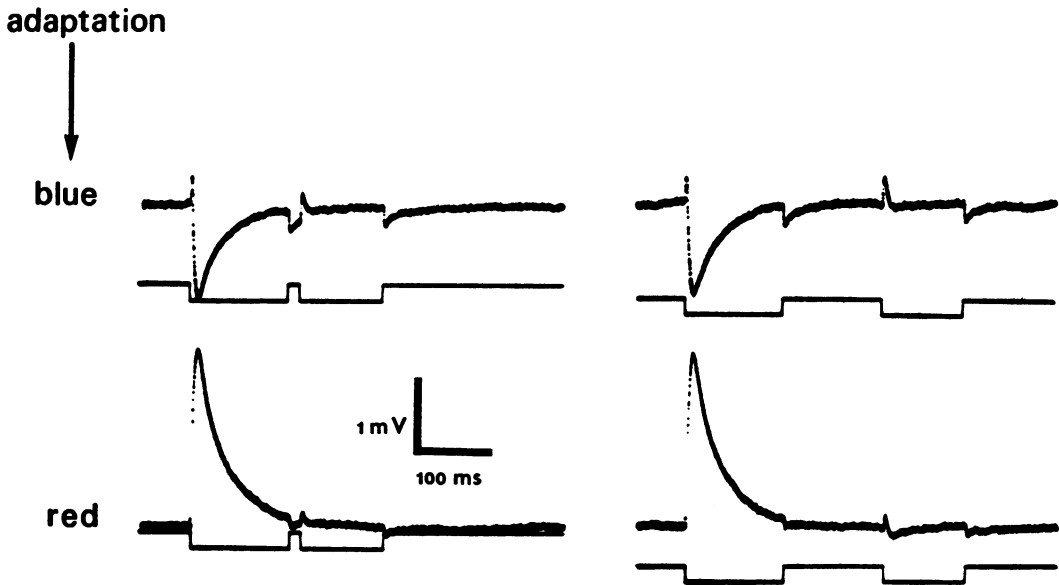
adaptation

FIGURE 8 Response shapes after partial recovery following blue and red adaptation. All four records were taken from one cell at 5°C. All responses are to maximum-intensity white-light stimuli given 30 s after blue (447 nm, 10 s) adaptation in the upper row, or red (K6, 10 s) adaptation in the lower row. The recovery time constant of the biphasic response is about 2 s in this cell after both red and blue adaptation. Note the difference in the negative "off" and positive "on" of the responses after blue adaptation compared with red adaptation. The figure shows that there is no fast transition from the D to the A state. It also shows the effect of a photochemical transition from a thermolabile state in the zero-latency negative off of all responses and in the zero-latency positive on of the upper and lower left responses to the second white stimulus.

white pulses following blue (upper traces) or red (lower traces) adaptation at 5°C, all in the same cell. In neither case is there any substantial recovery of either the positive or the negative ERP phases even after 250 ms; in fact longer dark times showed a recovery time constant of about 2 s for both the positive and the negative phases (Hillman et al., 1973). (The fast transition from the negative ERP subsystem to the D state is probably responsible for the small recovered positive phase seen in the upper traces.) Thus, there is a fast transition from the positive ERP subsystem only to F, that is $E \rightarrow F$. (We cannot allow $E \rightarrow B$ or $E \rightarrow C$ instead, for then we would see the slow time constant of the output of C following short white stimulation of the red-adapted cell as in Fig. 5, right.) Fig. 9 summarizes the results up to this point.

G. *Photochemical Transitions from Thermolabile States*

The "off" transients in Fig. 8 may be used to show the existence of two phototransitions from thermolabile states. In the lower pair of traces, the initial red adaptation,
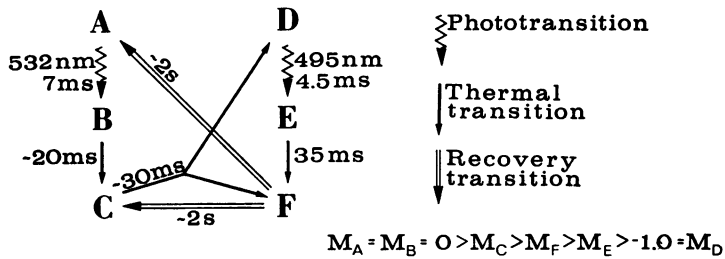
A   D   ‌Phototransition

532nm   495nm

7ms   4.5ms Thermal transition

B   E

-20ms   35ms Recovery transition

C   F

$M_A = M_B = 0 > M_C > M_F > M_E > -1.0 = M_D$

FIGURE 9 The minimal model needed to explain the observations of sections A–F.

according to the model developed so far, puts almost all the pigment in the D state. The following white pulses then transfer most to the F state, where it remains for the duration of the traces, since the thermal decay of F at this temperature takes seconds. The presence of an off transient therefore indicates a photo-output from F. (The size of the transient, though small, is quantitatively larger than could arise from the recovery-maintained population of D.) Since the transient is negative, the photo-induced dipole moment change must have been positive, that is, $F \rightsquigarrow A$, B, or C. However, C has a moment very near to that of F, and $B \rightarrow C$ is so fast that $F \rightsquigarrow B$ would look like $F \rightsquigarrow C$, so the transition is most likely $F \rightsquigarrow A$.

In the upper pair of traces of Fig. 8, the initial blue adaptation distributes the pigment between the A and D states. The white test flashes again put most of the pigment into the F state but this time with a substantial amount in C. The fact that the off transients in this case are considerably larger than in the lower traces then suggests the existence of a phototransition also out of C. By an argument similar to that of the preceding paragraph, $C \rightsquigarrow A$ is indicated.

The amplitudes of these transients are proportional to the products of light intensity, photosensitivity and population of state of origin, and dipole moment change in the transition. The population and dipole moment change, and therefore the photosensitivities, emerge from the quantitative calculation of the predictions of the model as described below.

There is a suggestion, from the observations of Figs. 8 and 11, of the existence of a further phototransition, $F \rightsquigarrow D$ but its influence is small and it has been omitted from further consideration at this stage.

This completes the transition model. The final model is shown in Fig. 10. However, certain parameters and constraints remain to be determined.

H. Additional Constraints and Parametric Determinations

The transitions whose rates remain undetermined are $C \rightarrow D$, $C \rightarrow F$, $F \rightarrow A$, and $F \rightarrow C$. $C \rightarrow D$ can be determined in principle from the growth of the positive response to a white test flash following saturated red stimulation of a blue-adapted cell (Fig. 7). The blue adaptation moves most of the pigment to state A, the red
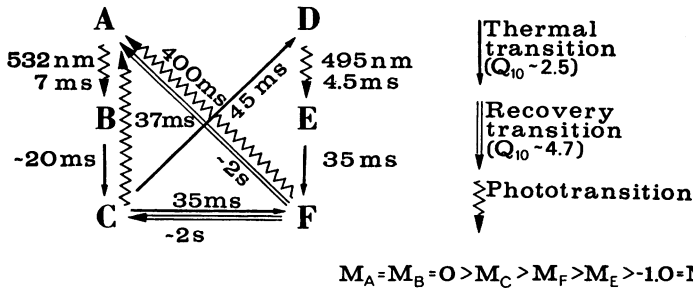
$$M_A = M_B = 0 > M_C > M_F > M_E > -1.0 = M_D$$

FIGURE 10 The "complete" model, but not including the parametric constraints and determinations of section H.

stimulation shifts it rapidly to C, and the white test flash determines the growth of D. Since we could not change filters sufficiently rapidly, however, we can (from this) put only an upper limit on the $C \rightarrow D$ time constant of about 100 ms.

With this fact, however, we can say that the "recovery" time constants of the positive and negative phases of the responses to white flashes following white bleaching are largely the time constants of $F \rightarrow C$ and $F \rightarrow A$, respectively. (Hillman et al., 1973, found these constants roughly similar; we find, by more accurate measurements, that they are in fact a little different in some cells—see Table III.)

Now the *ratio* of the dark populations of A and D following saturating white illumination is determined by the ratio $C \rightarrow F/C \rightarrow D$ together with the values of $F \rightarrow A$ and $F \rightarrow C$. The latter are measured as above and the population ratio is determined by decomposition of the biphasic response to a white test flash into its positive and negative components as detailed in Minke et al. (1973). We thus know $C \rightarrow F/C \rightarrow D$. Furthermore, from observations of the dark decay following the responses to short red flashes (Fig. 4) we know the decay time of C (see above). The reciprocal of this decay time is the sum of the reciprocals of the $C \rightarrow D$ and $C \rightarrow F$ times. From these two equations in $C \rightarrow D$ and $C \rightarrow F$, we can calculate $C \rightarrow D$ and $C \rightarrow F$ separately. However, the accuracy of the measurement of the decay time of C is poor, so these values serve only as rough limits for the computer calculation described in the next section, which fixes them much more accurately.

Finally, only the dipole moments remain undetermined (although constrained as shown in Fig. 10). In principle these too could be obtained directly from combinations of experiments, but their determination was found to be easier by varying them for best fit of the calculated curves to the corresponding responses—see next section.

The means of determining the model parameters are summarized in Table II.

I. *Computer Calculations*

For the six-compartment, two-stable-state model of Fig. 10, the differential equations presented in the Methods section reduce to the following set:

$$\dot{A} = -IX_{BA}A + IX_{AC}C + (k_{AF} + IX_{AF})F$$

$$\dot{B} = IX_{BA}A - k_{CB}B$$

$$\dot{C} = + k_{CB}B - (k_{DC} + k_{FC} + IX_{AC})C + k_{CF}F$$

$$\dot{D} = + k_{DC}C - IX_{ED}D$$

$$\dot{E} = + IX_{ED}D - k_{FE}E$$

$$\dot{F} = + k_{FC}C + k_{FE}E - (k_{AF} + k_{CF} + IX_{AF})F$$

$$A + B + C + D + E + F \equiv 1.$$

TABLE II

SUMMARY OF METHODS OF DETERMINING TRANSITION PARAMETERS

	Transition	Parameter	Observation from which parameter is derived	Figure	Section
Photo-transitions	$A \rightsquigarrow B$	X_{BA}	Time needed to run through the A-state population	2	C
	$D \rightsquigarrow E$	X_{ED}	Time needed to run through the D-state population	3	C
	$F \rightsquigarrow A$	X_{AF}	Size of the negative off-response to long white stimulation after red adaptation at low temperature*	8, 11, 13	G
	$C \rightsquigarrow A$	X_{AC}	Size of the negative off-response to long white stimulation after blue adaptation at low temperature*	8, 11, 13	G
Thermal transitions	$B \rightarrow C$	k_{CB}	Faster decay time constant of the negative ERP to a short red pulse after the cessation of the light	4	D
	$C \rightarrow D$ $C \rightarrow F$	k_{DC} and k_{FC}	(a) Slower decay time constant of the negative ERP to short red pulse after the cessation of the light; (b) Fraction of the positive phase in the biphasic ERP at low temperature (after knowing k_{CF} and k_{AF}) (Minke et al., 1973). A lower limit is set to k_{DC} from the fast transition time constant from the A state to the D state	4 7	D, F, H
	$E \rightarrow F$	k_{FE}	Decay time constant of the positive ERP to a short blue pulse after the cessation of the light	5	E
Recovery transitions	$F \rightarrow A$	k_{AF}	Negative ERP recovery time constant (Hillman et al., 1973)		B, H
	$F \rightarrow C$	k_{CF}	Positive ERP recovery time constant (Hillman et al., 1973)		B, H

* Evaluated by best fit of the calculated responses to the experimentally measured ones.

We have carried out a numerical calculation of the ERP predicted by these equations as explained in Methods, but subject to the following constraints:

Where the k's were measured directly, as described above, the measured values were initially used in the calculations. These values of course varied with temperature, but some also differed from cell to cell, though never by more than a factor 2. Furthermore, not all parameters were measured for each cell. The calculations were therefore done separately for each cell at each temperature, and the missing parameters were allowed to vary for best fit within this factor 2 of the average value in other cells. The measured parameters were also allowed to vary within their estimated experimental errors.

The same procedure was applied to the photochemical rate constants IX, except that, once fixed, the X's were assumed universal, that is, the same in all cells and at all temperatures.

The dipole moments were also assumed universal. They were not measured directly but were allowed to vary for best fit, subject to universality and the constraints detailed in Fig. 10.

A trial-and-error approach to the numerical calculation was used. That is, an initial set of measured and estimated (within the constraints) parameters was tried. The resultant curve was compared with the experimental response for the same paradigm, and the discrepancies—with some insight into which parameter affects what feature—were used to determine a new set of estimated parameters. The procedure was continued until a fit was obtained approximately as good as the variability of the response.

We note that in principle, an optimalization procedure could have been adopted, but the simpler trial-and-error technique was found adequate for present purposes. (It is possible that an optimalization procedure could have been used from the beginning to determine both the model and its parameters, but this approach has not been explored.)

The set of experimental paradigms to which fits were attempted was chosen to be as complex as possible—that is, to activate as strongly as possible, as many as possible of whatever transitions might be present. For this purpose, white stimuli (activating phototransitions at all wavelengths) and high intensities (populating thermolabile states as much as possible) were especially used. The effects of temperature, stimulus intensity, and color and duration of adaptation were also explored. A selection of experimental observations and the computer fits to them is shown in Figs. 11–14.

Fig. 11 illustrates the responses to pairs of white pulses of a cell adapted to blue or red light at low temperature and to red light at room temperature.

Figs. 12 and 13 give the responses to various intensities of white light in cells adapted to red or blue light, at room and low temperature, respectively. The increasingly rapid decay of the response with brighter stimuli arises from the emptying of the stable states.

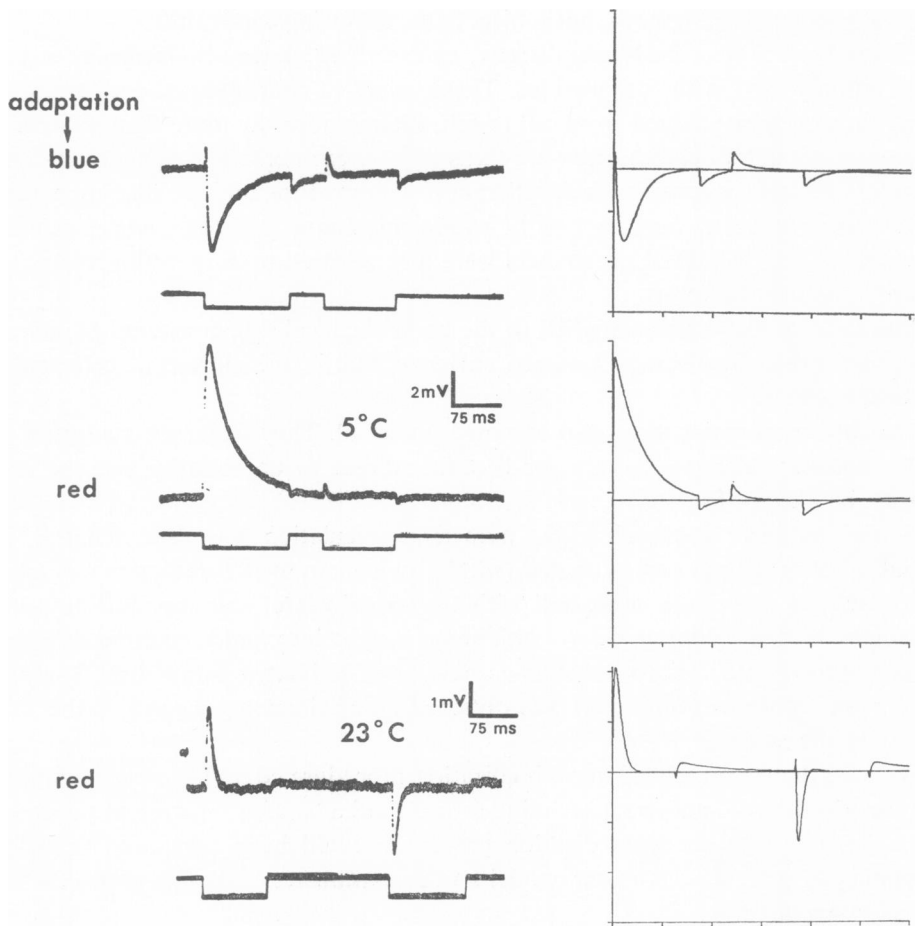Fig. 14 shows the responses at low temperature to identical brief white stimuli of a

FIGURE 11 Model computations of the responses to pairs of white pulses after blue and red adaptation. The left column shows the responses to pairs of maximum intensity white pulses 30 s after blue (447 nm, 10 s) adaptation (upper trace) or red (K6, 10 s) adaptation (lower two traces). The upper two traces are from one cell at 5°C and the bottom trace is from another cell at 23°C. The right column shows the responses calculated from the model for the experimental conditions of the corresponding left traces. The parameters used for this and the following figures are as listed in Table III.

cell adapted to a long or to a short white pulse (following long white adaptation). This illustrates that the final dark population distribution (determining the positive-to-negative response amplitude ratio) depends not only on wavelength but on time-intensity distribution of sufficiently intense adaptations. This is because imme-diately following brief intense light, most of the pigment is in state C, while for longer lights, the steady-state population is mainly in F.

Since the calculations were done by trial-and-error, the fits illustrated in Figs. 11–14 could undoubtedly be improved by minor parametric adjustment and the
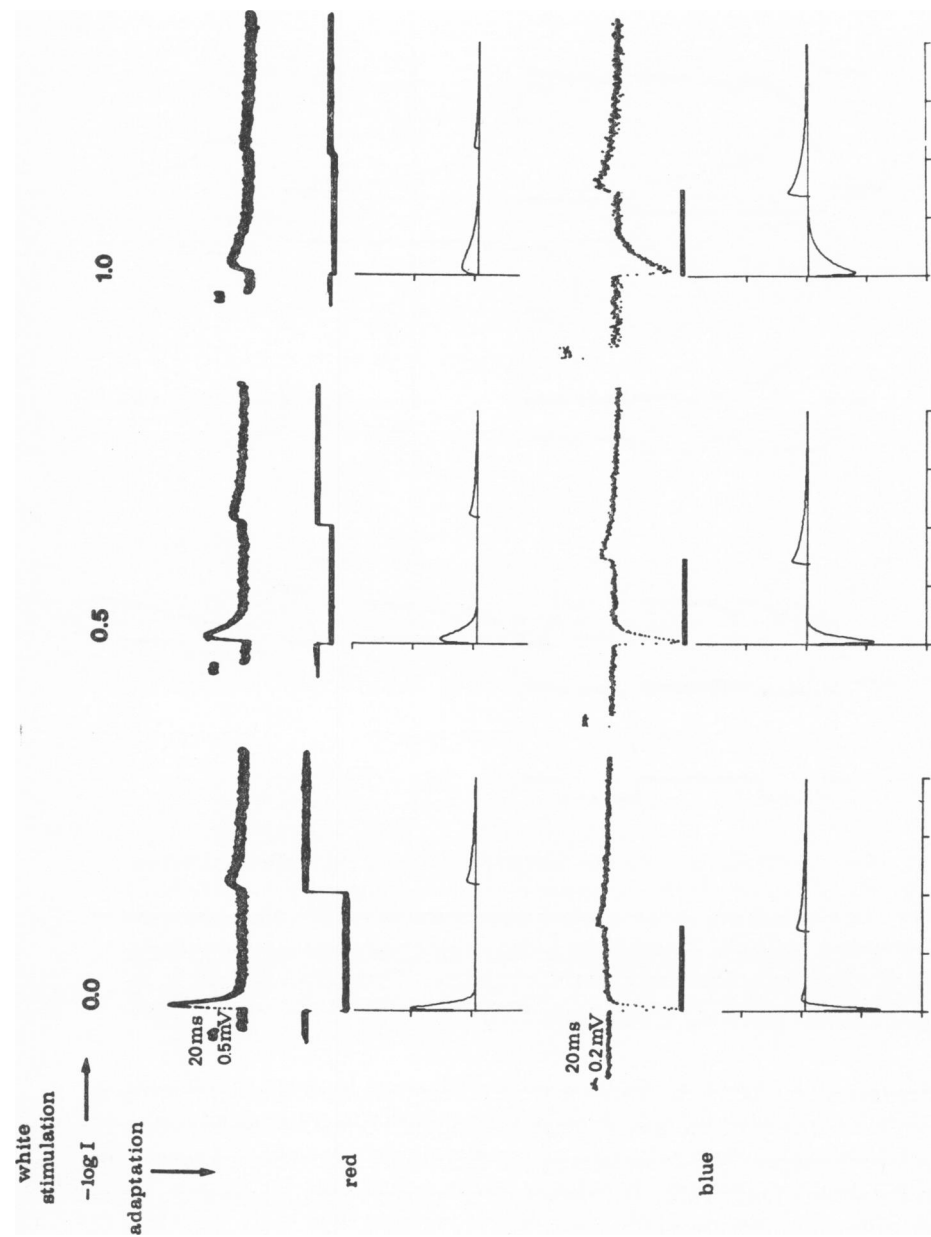
FIGURE 12 Model computations of responses to white light pulses at various intensities after blue and red adaptation at room temperature. The first and third rows are responses from one cell at 23°C to increasing white light stimulation (increasing left to right, as indicated above) 30 s after red (K6, 10 s) adaptation (first row), and after blue (447 nm, 10 s) adaptation (third row). The third row responses were averaged by a CAT (Computer of Average Transients) and their amplification varies as indicated by the calibration pulse. The horizontal bars below the third row responses indicate stimulus duration. The second and the fourth rows are the corresponding calculated responses at corresponding amplifications.
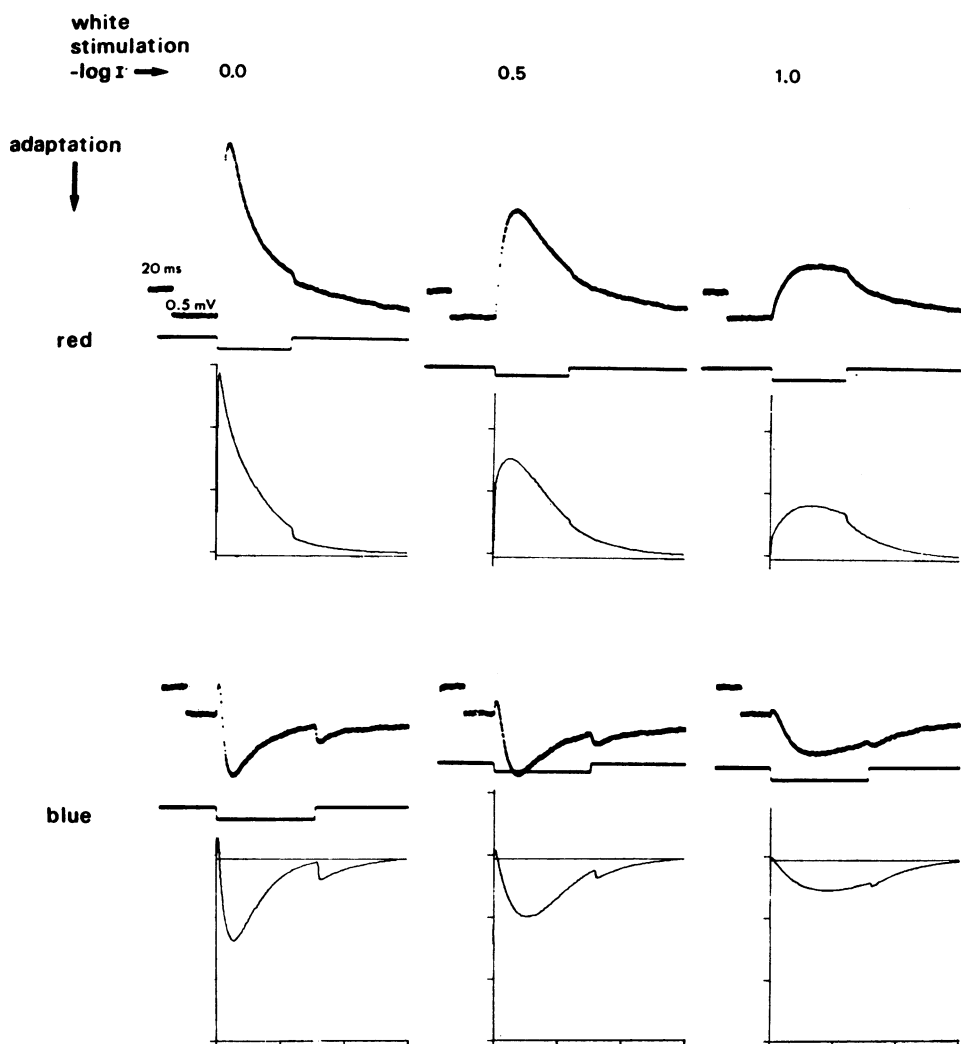
FIGURE 13 Model computations of responses to white light pulses of various intensities after blue and red adaptation at low temperature. The experimental procedure and figure representation are similar to Fig. 12 except that the temperature is 5°C. All responses are from one cell.

small discrepancies seen between experiment and theory are not considered to be an indication of inadequacy of the model (except as noted above).[2] It is clear that the fits are good and support the completeness of the model and the accuracy of the parametric determinations. Table III presents the values of the parameters determined as described here for four different cells.

---

[2] In some cells, there is a small residual LRP from the same cell or adjoining cells. This effect was particularly pronounced in the cells illustrated in Figs. 5 (top right) and 13, and is believed to be responsible for the slow final approaches to base line of the responses in these cells.

TABLE III
VALUES OF MODEL PARAMETERS USED IN CALCULATIONS*

Figure		Parameter										Initial fraction in D state	τ_m
	$1/IX_{BA}$	$1/IX_{BD}$	$1/IX_{AC}$	$1/IX_{AF}$	$1/k_{CB}$	$1/k_{FC}$	$1/k_{DC}$	$1/k_{FE}$	$1/k_{AF}$	$1/k_{CF}$		
11 First row	10.5	6.7	55	600	25	32	70	35	1,700	1,700	0.26	0.5
Second row	10.5	6.7	55	600	25	32	70	35	1,700	1,700	1.0	0.5
Third row	7	4.5	37	400	3	5	12	6	85	85	1.0	0.5
12 Red adaptation‡	7	4.5	37	400	2	4	6	7	80	180	1.0	0.5
Blue adaptation‡	7	4.5	37	400	2	4	6	7	80	180	0.18	0.5
13 Red adaptation‡	7	4.5	37	400	27	35	35	30	1,600	3,000	1.0	0.5
Blue adaptation‡	7	4.5	37	400	27	35	35	30	1,600	3,000	0.25	0.5
14 Trace B	10.5	6.7	55	600	34	40	40	30	2,600	3,000	0.31	2.0
Trace D	10.5	6.7	55	600	34	40	40	30	2,600	3,000	0.36	2.0

	M_A	M_B	M_C	M_D	M_E	M_F
All	0.00	0.00	-0.30	-1.00	-0.43	-0.24

* $1/IX$, $1/k$, and τ_m in milliseconds, M in arbitrary units.

‡ Values of IX are for $-\log I = 0$ white light and must be multiplied by 3.2 and 10 for $-\log I = 0.5$ and 1.0, respectively.
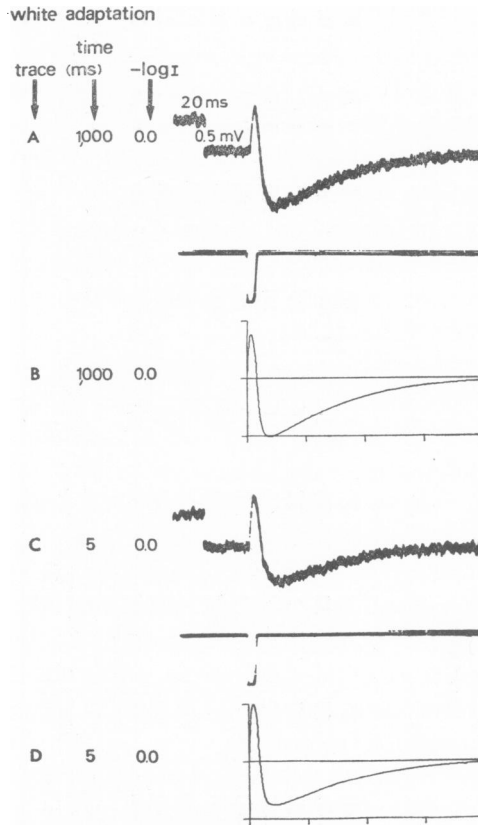
FIGURE 14 The dependence of the response shape on the duration of the adapting light. Traces A and C are responses of one cell to identical maximum intensity white light stimuli at 3°C. 60 s before stimulation in traces A and C the cell received 5 s maximum intensity white-light adaptation. 30 s later the cell received 1 s additional white-light adaptation in trace A and 5 ms white-light adaptation in trace C. The figure shows that the positive phase is bigger and the negative phase is smaller after short pulse adaptation. Traces B and D are the corresponding calculated responses. A calculation shows that the population of the D state is 5% greater after short-pulse adaptation than after long-pulse adaptation.

The Q_{10}'s quoted in Fig. 10 are only approximate, but the following observation shows that (barring accidental cancellation of opposing effects) $Q_{10}(F \rightarrow C) = Q_{10}(F \rightarrow A)$ and $Q_{10}(C \rightarrow F) = Q_{10}(C \rightarrow D)$. We recall that the positive phase of the low-temperature response to a white light arises from activation of D and the negative phase from A. This low-temperature response was observed following white adaptation at low temperature and at high temperature. The two responses were identical, indicating that the A/D population radio resulting from a given adaptation is independent of the temperature at which the cell was adapted. Since A/D is determined by the rate constant ratios k_{CF}/k_{AF} and k_{FC}/k_{DC} these latter are apparently also independent of temperature.

IV. CONCLUSIONS

We have demonstrated that careful exploitation of a single approach based on early receptor potential recordings is capable of producing a fairly complete and quantitative model for the states and transitions of a visual pigment *in situ*. Nevertheless, it is clear that other techniques should be used to confirm and supplement the results. For instance, transitions which involve little change of dipole moment (such as $A \rightarrow B$ in our model) can be inferred only indirectly from ERP observations, while they would be directly seen photometrically if they involved appreciable changes of spectral absorption. Spectrophotometry is of course correspondingly insensitive to transitions involving little spectral change.

In attempting a comparison with existing pigment models, we note that no model of comparable completeness exists for any invertebrate photoreceptor (see Hagins and McGaughy, 1967; and Morton, 1972). Detailed vertebrate models exist (Morton, 1972), but are so dissimilar to the present model (including no second stable states no double cycle, and no room-temperature time constants between a few milliseconds and many seconds [Abrahamson and Wiesenfeld, 1972]) as to make assignments of corresponding states, in the absence of spectral and biochemical examination, not only hazardous but probably misleading. Minke et al. (1973) suggested that our states A and D might be rhodopsin and a metarhodopsin, respectively. The following circumstantial evidence supports this conclusion: (*1*) The transition of pigment from state A to state D induces excitation (Hochstein et al., 1973) as does the transition from rhodopsin to metarhodopsin in other preparations (octopus *Eledone moschata*, neuropter *Ascalaphus macaronius*, moth *Deilephila elpenor*, and fly *Calliphora erythrocephala* [Hamdorf et al., 1973]; fruit fly *Drosophila* [Pak, W. L., and S. E. Ostroy, 1974, private communication]). (*2*) State D has a greater photosensitivity than state A, as does metarhodopsin in these other preparations. (*3*) The absorption spectrum wavelength shift from A to D is similar to that of rhodopsin to metarhodopsin in other crustacea (Goldsmith, 1972).

Without biochemical examination, it is also difficult to suggest which transitions are exothermic and which are endothermic—that is, involve metabolic energy. The slow ("recovery") transitions $F \rightarrow A$ and $F \rightarrow C$ (also having Q_{10}'s different from those of the remaining transitions) are probably the best candidates for metabolically supported transitions.

REFERENCES

ABRAHAMSON, E. W., and J. R. WIESENFELD, 1972. *In* Handbook of Sensory Physiology. H. J. A. Dartnall, editor. Springer-Verlag, Berlin. **7** (Pt. 1): 69.

ARDEN, G. B., H. IKEDA, and I. M. SIEGEL. 1966. *Vision Res.* **6**:373.

BROWN, P. K., and R. H. White. 1972. *J. Gen. Physiol.* **59**:401.

CONE, R. A. 1963. *J. Gen. Physiol.* **46**:1267.

CONE, R. A. 1967. *Science (Wash. D. C.).* **155**:1128.

DARTNALL, H. J. A. 1972. *In* Handbook of Sensory Physiology. H. J. A. Dartnall, editor. Springer-Verlag, Berlin. **7** (Pt. 1): 122.

EBREY, T. G. 1968. *Vision Res.* **8**:965.

GOLDSMITH, T. H. 1972. *In* Handbook of Sensory Physiology. H. J. A. Dartnall, editor. Springer-Verlag, Berlin. **7** (Pt. 1):685.

HAGINS, W. A., and R. E. McGAUGHY. 1967. *Science (Wash. D. C.).* **157**:813.

HAMDORF, K., R. PAULSEN, and J. SCHWEMER. 1973. *In* Biochemistry and Physiology of Visual Pigments. H. Langer, editor. Springer, New York. 155.

HILLMAN, P., F. A. DODGE, S. HOCHSTEIN, B. W. KNIGHT, and B. MINKE. 1973. *J. Gen. Physiol.* **62**:77.

HOCHSTEIN, S., B. MINKE, and P. HILLMAN. 1973. *J. Gen. Physiol.* **62**:105.

KROPF, A. 1972. *In* Handbook of Sensory Physiology. M. G. E. Fuortes, editor. Springer-Verlag, Berlin. **7** (Pt. 2):239.

MAINSTER, M. A., and T. J. WHITE. 1972. *Vision Res.* **12**:805.

MINKE, B., S. HOCHSTEIN, and P. HILLMAN. 1973. *J. Gen. Physiol.* **62**:87.

MORTON, R. A., 1972. *In* Handbook of Sensory Physiology. H. J. A. Dartnall, editor. Springer-Verlag, Berlin. **7** (Pt. 1):33.

PAK, W. L., and R. BOES. 1967. *Science (Wash. D. C.).* **155**:1131.